Experimed 2022; 12(3): 188-201

ORIGINAL ARTICLE

DOI: 10.26650/experimed.1188586

Differential Cytotoxic Activity of a New Cationic Pd(II) Coordination Compound with N_4-Tetradentate Hybrid Ligand in Cancer Cell Lines

Merve Erkisa Genel[1, 2, 3], Selin Selvi[3], Ismail Yilmaz[4], Remzi Okan Akar[3, 6], Ilhan Yaylim[1], Abdurrahman Sengul[5,*], Engin Ulukaya[3,6,*]

*asterik indicates two corresponding authors

[1]Department of Molecular Medicine, Aziz Sancar Institute of Experimental Medicine, Istanbul University, Istanbul, Turkiye

[2]Institute of Graduate Students in Health Sciences, Istanbul University, Istanbul, Turkiye

[3]Molecular Cancer Research Center (ISUMKAM), Istinye University, Istanbul, Turkiye

[4]Department of Chemistry, Faculty of Science, Karabuk University, Karabuk, Turkiye

[5]Department of Chemistry, Faculty of Arts and Sciences, Zonguldak Bulent Ecevit University, Zonguldak, Turkiye

[6]Department of Clinical Biochemistry, Faculty of Medicine, Istinye University, Istanbul, Turkiye

ORCID ID: M.E.G. 0000-0002-3127-742X; S.S. 0000-0003-2762-4780; İ.Y. 0000-0002-0139-0122; R.O.A. 0000-0001-8687-2034; İ.Y. 0000-0003-2615-0202; A.S. 0000-0001-6851-4612; E.U. 0000-0003-4875-5472

Cite this article as: Erkisa Genel M, Selvi S, Yilmaz I, Akar RO, Yaylim I, Sengul A, Ulukaya E. Differential cytotoxic activity of a new cationic Pd(II) coordination compound with n4-tetradentate hybrid ligand in cancer cell lines. Experimed 2022; 12(3): 188-201.

ABSTRACT

Objective: Successful cancer treatment still requires the discovery of novel compounds that hold promise for chemotherapeutics. The objective of this study was to examine the effectiveness of a newly synthesized cationic palladium(II) coordination compound that functions via several pathways to provide an efficient therapeutic option for various cancer cells.

Materials and Methods: A new cationic palladium(II) coordination compound, [Pd(**L**)]$Cl_2 \cdot H_2O$, denoted as Complex 1, where the ligand L is the compound 6,6'-bis(NH-benzimidazol-2-yl)-2,2'-bipyridine), was synthesized and characterized by the attenuated total reflectance (ATR) - fourier-transform infrared spectroscopy (FT-IR), proton nuclear magnetic resonance (^{1}H NMR), electrospray ionization mass spectrometry (ESI-MS), and carbon-hydrogen-nitrogen (CHN) analyses. The density functional theory (DFT) calculations show the coordination sphere around the metal center in Complex 1 to be made up of tertiary N atoms of the pyridine (py) and benzimidazole (bim) rings completing the square-planar geometry with significant distortion. The anti-growth/cytotoxic activity of the complex was determined using the sulforhodamine B (SRB) and adenosine triphosphate (ATP) viability assays for 24 and 48 h *in vitro*. The study evaluates the determinations for annexin V-propidium iodide (PI) positivity, mitochondrial membrane potential loss, Bcl-2 protein inactivation, and deoxyribonucleic acid (DNA) damage to investigate the cell death mode and its partial mechanism.

Results: Complex 1 caused cytotoxicity in a dose-dependent manner in all the cell lines used, with IC_{50} values ranging from 2.6-8.8 μM for 48 h. Among the cancer models, colon and breast cancer cell lines underwent cell death by well-described apoptosis through the intrinsic pathway involving the mitochondria. However, the other cell lines did not show such a cell death modality. This implies that differential cell death modes operate based on the cancer type.

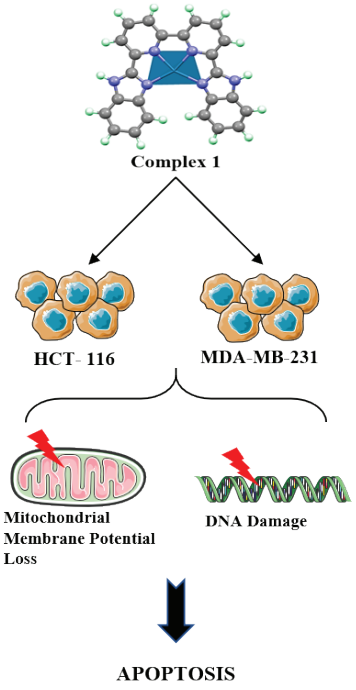
Conclusion: For the treatment of breast and colon cancers, the complex 1 appears to be a unique, promising complex. Therefore, complex 1 deserves further attention for proof of concept in animal models.

Keywords: Palladium complexes, N4-donor ligand, benzimidazole, bipyridine, apoptosis, anticancer effect

Corresponding Author1: Engin Ulukaya **E-mail:** eulukaya@istinye.edu.tr
Corresponding Author2: Abdurrahman Sengul **Email:** sengul@beun.edu.tr
Submitted: 14.10.2022 **Revision Requested:** 26.10.2022 **Last Revision Received:** 03.12.2022 **Accepted:** 05.12.2022 **Published Online:** 27.12.2022

Content of this journal is licensed under a Creative Commons Attribution-NonCommercial 4.0 International License.

GRAPHICAL ABSTRACT



Highlights

- A new cationic Pd(II) complex is synthesized with N_4-donor ligand
- DFT calculations show that complex 1 has a distorted square planar geometry
- Complex 1 dependent cell death mode differs depending on the type of cancer.
- Complex 1 induces intrinsic apoptosis and DNA damage in colon and breast cancer cells.

INTRODUCTION

Successful cancer treatment still needs new complexes to be developed that hold promise for chemotherapeutics due to a few reasons such as acquired resistance to anticancer drugs during the treatment period with few exceptions. Another problem is the heterogeneity of tumor tissue, the presence of a variety of clones in the same tissue that respond differently to the applied treatments. Another important problem is the serious side effects of the drugs, sometimes even resulting in discontinued treatment. Therefore, developing novel compounds would provide a chance at gaining a new set of anticancer drugs. These may even have a new class of mechanisms of action that will be profoundly appreciated. Metal-based complexes (e.g., cisplatin) are particularly efficient in terms of their DNA-damaging effects that eventually cause cell death. Since the discovery of cisplatin (i.e., cis-diamminedicholorplatinum II, or cis-[$Pt(NH_3)_2Cl_2$]), countless research advances have been performed for preventing and treating cancer. Chemotherapeutic drugs that are currently on the market have poor efficacy and harmful side effects (1). Therefore, a focus in this particular discipline involves the creation and development of new anticancer medications with greater cytotoxic efficacy against cancer cells and minimal side effects. Due to their capacity to interact with a variety of different enzymes and receptors, benzimidazoles are well known as biologically significant chromophores in medicinal chemistry (2). Transition metal complexes of such biologically significant ligands exhibit better pharmacological activity than the corresponding free ligand.

Studies of transition metal coordination complexes with N_4-donor tetradentate ligands are appealing due to their interesting coordination modes, catalytic activities, and electronic and photo-physical properties (3, 4). In particular, square-planar d^8 metal complexes with these types of ligands have gained enormous interest in the field of anticancer drug agents due to these planar metal complexes providing a large aromatic surface as a prerequisite for DNA intercalators (5). Cisplatin is one of clinics' most effective and widely used chemotherapeutic agents. However, cisplatin causes serious side effects like nephrotoxicity, ototoxicity, nausea, and vomiting. Due to its limited efficacy and severe side effects, researchers are focused on developing new platinum drugs that have fewer side effects and the ability to overcome drug resistance (6). Although intense research on the biological activities of metallointercalators has been performed, the intrinsic relationship between their molecular structure and cytotoxicity has yet to be elucidated. Researchers aim to modify the structure of the intercalator ligand to develop new drugs possessing different biological activities. In this respect, studies have shown that changing the metal ion and modifying the organic ligand in the coordination complexes results in the changes in the DNA affinity, binding mode, and strength of the transition metal complexes (7). Even though palladium and platinum are members of the same chemical group, their modes of action may be distinct from those of cisplatin and from one another. In comparison to their Pt(II) counterparts, Pd(II) complexes have a stronger capacity to coordinate with DNA bases and, as a result, more effectively suppress the proliferation of cancer cells such as KB, A549, and MCF7 (8). When coupled with N-donor ligands, Pd(II) and Pt(II) assume the same square-planar geometry and exhibit similar properties as a d^8-metal ion. The Pt(II) is kinetically more stable than the Pd(II) counterpart as revealed by the ligand-exchange kinetics during the aquation reaction Pd(II) estimated to be 10^6 times faster than Pt(II) (9). As a tridentate chelating ligand, 2,6-bis(NH-benzimidazol-2-yl)pyridine coordinates with the metal center stronger than the tridentate 2,2':6',2"-terpyridine ligand due to the benzimidazole rings being more basic than the pyridine rings (10). Therefore, the present complex of the N_4-donor hybrid ligand which acts as a π-donor and π-acceptor can be compared to analogous metal complexes with QP, such as $(Pt(QP))^{2+}$ which has been shown to bind to double-helix DNA more strongly than the terpyridine (terpy)- and bipyridine (bpy)-Pt(II) complexes (11). The DNA binding of the substrate depends

on the surface extension of the aromatic moiety. The Pt(II) complex (i.e., $Pt(QP)^{2+}$) was demonstrated to have comparable cytotoxicity to cisplatin against human carcinoma cell lines (e.g., breast, colorectal, lung), and cisplatin-resistant cell lines (5). As previously established, metal complexes' biological activity can be regulated by changing the metal ion and modifying the ligand structure through the introduction of NH functionalities along with the extension of the aromatic ring system, as exemplified by the study from Chi-Ming Che et al. (12). In this regard, the current study would like to report the synthesis of a new Pd(II) coordination complex with a tetradentate 2,2'-bipyridine ligand bearing biologically significant benzimidazole chromophores that extends the aromatic surface and provides NH functional groups for hydrogen bonding interactions with DNA (13, 14). Also, the ligand (**L**) having an N_4-tetradentate binding pocket, which forms a stable chelate $(Pd(\mathbf{L}))Cl_2{\cdot}H_2O$ under physiological conditions, is expected to show higher cytotoxic activity as has been observed for the polypyridine-iron(II) complexes (15). Such structural and chemical properties of the new cationic palladium(II) complex are significantly important for a potential drug targeting DNA due to the present *in vitro* studies of the platinum(II) counterpart having been found to exhibit higher cytotoxic activity in comparison to cisplatin toward certain cancer lines (14). In present study has found the Complex 1 to show promise toward prostate cancer treatment with an IC_{50} value of 2.6 μM, which deserves further attention from proof-of-concept studies.

MATERIALS AND METHODS

Materials

Analytical pure reagents were obtained from Merck. IR spectra were analyzed in the 4,000-600 cm^{-1} region using PerkinElmer Spectrum 100 fourier-transform infrared (FT-IR) spectrophotometer. Nuclear magnetic resonance analysis (NMR) results were obtained using the Bruker DPX-400 NMR spectrometer. Analysis of the elements was carried out on the element analyzer. Liquid chromatography-mass spectrometry/mass spectrometry (LC-MS/MS), electrospray ionization mass spectrometry (ESI-MS) were obtained with an AB 4000 QTRAP LC-MS. $Pd(COD)_2Cl_2$ where COD = 1.5-cyclooctadiene was prepared according to the methods in the literature (15). Ground-state geometry optimization was studied as described elsewhere (16, 17). The software Gaussian 09 was used for calculations and the software Gaussview 5.0 was used for visualizations (18). The B3LYP/6–31G(d,p) level was chosen because the B3LYP functionality has been proven to give good results for organic molecules (19) and the LANL2DZ basis set for the metal coordination compound. A similar previous study discovered the B3LYP/6-31G(d,p) level results to correlate with the experimental data (20).

Synthesizing the Ligand 6,6′-bis(NH-benzimidazol-2-yl)-2,2′-bipyridine (L)

The synthesis and purification details of the ligand have been previously reported (14, 21), and the characterization data are identical with the literature data (14). ESI-MS: *m/z* 411.1 $[M+Na]^+$ (Figure S1). ^1H NMR (DMSO-d_6): δ = 13.09 (s, 2H, NH), 9.09 (d, 2H, J = 7.83 Hz, bpy-H3,3'), 8.54 (d, 2H, J = 7.76 Hz, bpy-H5,5'), 8.26 (t, 2H, $J_{4,5}$ = 7,80 Hz, $J_{4,3}$ = 7,82 Hz, bpy-H4,4'), 7.76 (d, 2H, J = 8 Hz, bim), 7.66 (d, 2H, J = 8 Hz, bim), 7.30 (m, 4H, bim) (Figure S2). ^{13}C NMR (DMSO-d_6): δ = 155 (bpy-C2,2'), 152 (bim-C2,2'), 148 (bpy-C6,6'), 144 (bim), 139 (bpy-C4,4'), 124 (bpy-C3,3'), 123 (bim), 120 (bpy-C5,5') ve 113 (bim) (Figure S3). Attenuated total reflectance (ATR)-FT-IR (4000-600 cm^{-1}): 3286 (br, w, ν_{as}(N-H), 3074 (w, ν_{as} Ar-H), 1657(m), 1624(m), 1589(m), 1573(m) (bim and py rings), 1434 (br, s, δ (N-H), 1371 (s, δ CH)), 1231(s, ν(C-N)), 1079 (s), 991(m), 935 (m), 877 (m), 808 (m), 741 (s, δ (C-H)) (Figure S4).

Synthesizing the 6,6′-bis(NH-benzimidazol-2-yl)-2,2′-bipyridylpalladium(II)chloride Monohydrate $[Pd(L)]Cl_2{\cdot}H_2O$

The mixture of $[Pd(L)]Cl_2{\cdot}H_2O$ (0.019 g, 0.065 mmol) in MeOH was mixed with a solution of 6,6′-bis(NH-benzimidazol-2-yl)-2,2′-bipyridine (0.003 g, 0.065 mmol) in MeOH (25.0 mL) (25.0 mL). The reaction solution was mixed for 3 h at reflux. The yellow solid that precipitated at room temperature was then filtered and air dried (22 mg, 60% humidity) after washing with about 200 mL of methanol and diethyl ether, respectively. Analysis calculated for $C_{24}H_{16}N_6Cl_2Pd{\cdot}H_2O$: C 49.48; H 3.11; N 14.44. Found: C 49.52; H 2.98; N 14.55. FT-IR (KBr, ν/cm^{-1}): 3427 (w, ν_{as}(N-H)), 3067 (w, ν (Ar-H), 1592 (m) and 1570 (s) (py and bim rings), 1457 (s), 1411(s), 1271 (s), 812 (s), 735 (s), 708 (m) (Figure 1). LC-ESI-MS *m/z* 246 $[Pd(\mathbf{L})]^{2+}$, 389 $[\mathbf{L}+Na]^+$, 495.4 $[Pd(\mathbf{L})-H]^+$, 554.9 $[Pd(\mathbf{L})+Cl+Na]^+$ (Figure S5). ^1H NMR (DMSO-d_6): δ = 14.15 (brd, s, NH), 9.11 (d, J = 8 Hz, 2H), 8.45 (d, J = 8 Hz, 2H), 8.29 (t, J = 8 Hz, 2H), 7.74 (m, 4H), 7.34 (m, 4H) (Figure S6).

Cell Culture

The A549, MDA-MB-231, PC-3, HCT-116, and BEAS-2B cell lines were cultured in the RPMI 1640 (Gibco, Grand Island, NY, USA) medium supplemented with 100U/mL penicillin+100μg/mL streptomycin (P/S; Gibco, Grand Island, NY, USA), 2 mM L-glutamine (Gibco, Grand Island, NY, USA), and a 10% fetal bovine serum (FBS; Lonza, Verviers, Belgium). MDA-MB-231 cells were cultured in the RPMI-1640 medium supplemented with P/S, 2 mM L-glutamine, and 5% FBS. All cells were incubated at 37°C in a humidified atmosphere containing 5% CO_2.

Determination of the Antiproliferative Effect Using the SRB and ATP Viability Assays

For the sulforhodamine B assay (SRB; Invitrogen S1307, Massachusetts, USA) and the adenosine triphosphate assay (ATP ; SIGMA 32160414, Missouri, USA) assays, all cells were cultured at a density of $5{\times}10^3$ cells per well on a 96-well plate in triplicates. After 24 h, Complex 1 was added at different concentrations (Range = 1.25-40 μM) over 48 h. After the treatment period, the SRB and ATP assays were studied, as described elsewhere (14).

Evaluation of the Cell Death Using Flow Cytometry

To specify Complex 1's effects on apoptosis, the study measured γ.H2A.X (phosphorylation of the Ser-139 residue of the histone variant (H2A.X)) activation (MCH200101 Millipore, Darmstadt,

Germany), the MitoPotential assay (MCH100110, Millipore, Darmstadt, Germany), Bcl-2 inactivation (MCH200105, Millipore, Darmstadt, Germany), and phosphatidylserine translocation (MCH100105, Millipore, Darmstadt, Germany) using flow cytometry. All cell lines were seeded at $3x10^5$ cells/well into 6-well plates and treated with Complex 1 at the previously calculated IC_{90} values and incubated for 24 and 48 h. At the end of the treatment period, all of the assays were implemented as described to the cells (22).

Statistical Analyses

GraphPad Prism 6.0 statistical software (San Diego, CA) for Windows was used to perform one-way ANOVA on all of the data before the Tukey post-hoc test. Statistical significance was defined as $p < 0.05$.

RESULTS AND DISCUSSION

Geometry Optimization

The geometry-optimized structure of Complex 1 has been obtained through density functional theory (DFT) calculations with the exception of the crystallization water and the counter ion chlorides (Figure 1). Table S1 gives the selected bond distances, angles, and dihedral angles for the optimized metal Complex 1. The palladium(II) ion in Complex 1 is seen to have adopted a distorted square-planar geometry with a N_4-donor tetradentate ligand akin to that of the structurally related coordination compound 2,2':6',2":6",2"'-quaterpyridine (QP) with platinum(II), $[Pt(QP)]^{2+}$ (23). The Pd atom in Complex 1 deviates by 4.7° from the square planar geometry (Figure 3a). Bipyridine and benzimidazole moieties are not coplanar (Figure 3b). The mean planes of the two bim rings intersect at 9.7° (the difference between C17-N2-Pd-N4 and C18-N5-Pd-N4), and the dihedral angle between the py and bim rings is nearly 176.8° (N4-C1-C24-N6), with bond lengths and bond angles being affected by these deviations. Pd-N bond lengths on the bim side (Pd-N2 and Pd-N5) are longer than Pd-N bond lengths on the py side (Pd-N3 and Pd-N4 in Table 1). The trans angles N2-Pd-N4 and N3-Pd-N5 are 159.12°, indicating a distorted square geometry. As far as the study has noted, this seems to be the first palladium(II) complex with the N_4-donor 6,6'-bis(NH-benzimidazol-2-yl)-2,2'-bipyridine ligand.

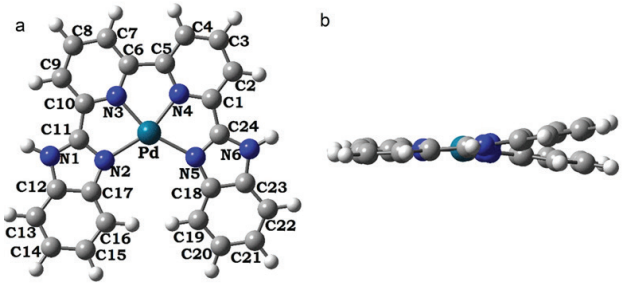
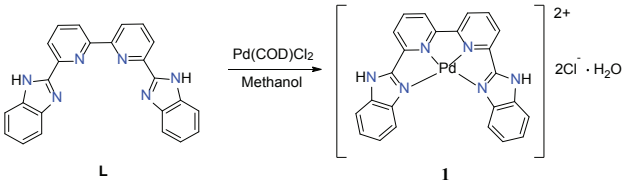


Figure 1. Optimized gas-phase structure of Complex 1 at B3LYP/6-31G(d,p) level with LANL2DZ on metal (a: top view, b: side view)

Synthesis and Characterization

The N_4-donor tetradentate hybrid ligand (**L**) was synthesized as reported previously (21), with the specifics of the synthesis and characterization of the ligand having been recently detailed (24). The characterization data for **L** are identical to those of the reported data (24). The ESI-MS spectrum (Figure S1) shows the molecular ion peak at *m/z* 411.1 to be attributed to $[L+Na]^{+\cdot}$.

The Pd(II) coordination Complex 1 was readily obtained by the treatment of $[Pd(COD)Cl_2$ with **L** in refluxing methanol at good yield, as illustrated in Scheme 1. The compound dissolves in



Scheme 1. The synthetic route of the palladium(II) complex

the coordinating solvents of DMF and DMSO, but is insoluble in common solvents. All attempts to obtain single crystals of Complex 1 were met with failure. The elemental analysis of Complex 1 offered a 1:1 (metal:ligand) stoichiometry, as expected, For Complex 1, a water molecule was added as a result of the analytical findings supporting this (*vide infra*).In the mass spectrum of Complex 1 (Figure S5), the mono-charged ion at *m/z* 495.4 corresponds to $[Pd(\mathbf{L})-H]^+$ ($C_{24}H_{17}N_6Pd$). The low-intensity parental peak at *m/z* 246 corresponds to the doubly charged ion $[Pt(\mathbf{L})]^{2+}$, thus confirming the proposed cationic structure as depicted in Scheme 1. The peak at *m/z* 554.9 corresponds to $[Pd(\mathbf{L})+Cl+Na]^+$ ($C_{24}H_{16}N_6ClPdNa$) and agrees well with the molecular structure. The peak corresponding to the ligand is observed at *m/z* 381.6.

NMR Study

The ^1H NMR (Figure S2) and ^{13}C NMR (Figure S3) spectra of **L** are included for a better comparison with the corresponding palladium(II) Complex 1. The proposed structure is perfectly compatible with the 1H NMR spectra of L. The N-H proton signals appear at 13.09 ppm as a singlet. The protons on the py rings resonate at 9.09 ppm (2H, doublet), 8.54 ppm (2H, doublet), and 8.26 ppm (2H, triplet), respectively. The protons on the benzene rings are observed at 7.76 ppm (2H, doublet), 7.66 ppm (2H, doublet), and 7.30 ppm (4H, multiplet), respectively. The molecule holds the C_2 symmetry in solution, indicating the bim rings to be magnetically equivalent. This is further confirmed by the ^{13}C NMR spectrum, which shows five different C atoms on the py ring and four different C atoms on the bim ring, as illustrated in Figure S6. The metal complex's 1H NMR spectra has been provisionally assigned due to not being well-resolved. The ^1H NMR spectrum (Figure S6) shows the N-H signal at 14.15 ppm as a broad singlet, which is the most deshielded in comparison to that of the free ligand (13.09 ppm). The rise in the N-H acidic character upon coordination of

the benzimidazole ring to the palladium(II) center through the imine N atoms is attributed to the substantial downfield shift in the bim N-H signal. The signals of the 2,2'-bipyridine protons appear in the expected pattern and region as observed for the free ligand. The three signals observed at 9.11 ppm as a doublet for H3,3', 8.45 ppm as a doublet for H5,5' and 8.29 as a triplet for H4,4' indicate the molecule to have adopted a C_2 symmetry in solution. The bpy protons show insignificant shifts compared to those of the free ligand. The benzene protons seem unaffected by the coordination. The benzene protons resonate in the same region (7.7-7.3 ppm) observed for the free ligand.

FT-IR Spectra

Figure S4 depicts the IR spectra of the substance **L**. The presence of intermolecular hydrogen bonds between the benzimidazole rings in the molecule is shown by the extensive absorption in the range of 3,600-2,400 cm^{-1} (25). According to the predictions made for a polar molecule with strong H-bond donor and acceptor groups that easily interact with the polar solvent, this broad absorption encompasses the OH stretching of the hydration water. The O-H bending overtone of water can be responsible for the extra dip at around 3,200 cm^{-1} (26). No absorption occurs corresponding to the free O-H stretches of water above 3,600 cm^{-1}. The frequency at 1,589 cm^{-1} may be assigned to the N-H in-plane bending mode (25). The aromatic ring's C-H stretching vibration is blamed for the weak absorption at 3,074 cm^{-1}. The frequencies at 1,573 and 1,522 cm^{-1} can be assigned to the stretching of the bim and py rings (27). The absorptions between 900 and 600 cm^{-1} are mostly due to the C-H out-of-plane and N-H out-of-plane bends as well as the in-plane ring bending modes.

R spectroscopy can be used to gain a better understanding of how the ligand and metal coordinate. Comparing the IR spectra of the complexes to those of the free ligands reveals noteworthy differences. The FT-IR (Figure 3) further supports the existence of the hydrated complex by showing broad bands in the range of 3,500-2,400 cm^{-1} that are caused by intermolecular hydrogen bonds between the benzimidazole N–H. The N-H stretching peak at 3,427 cm^{-1}, which is sharper than that of the unbound ligand, may be an indication of the N-H groups not being engaged in the coordination. The characteristic aromatic CH stretching is observed at 3,067 cm^{-1}, and those related to the benzimidazole and pyridine ring stretching modes are observed in the region of 1,591-1,411 cm^{-1}. Except for minor changes in their locations and intensities brought on by coordination, the other bands in the complex's spectra are essentially identical to those in the spectrum of the ligand. The peaks at 1,570 and 734 cm^{-1} in Complex 1 are stronger and sharper than the corresponding peaks at 1,573 and 741 cm^{-1} in the free ligand. This may imply Complex 1 to have a more rigid structure compared to the flexible ligand showing N-H tautomerism.

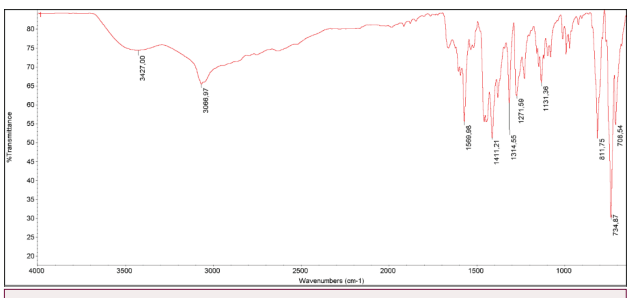


Figure 3. FT-IR spectra of Complex 1.

Effect of the Complex on Cell Viability

First, the study examined the cytotoxic effects of Complex 1 on the four most prevalent human cancer cell lines (i.e., A549, lung; MDA-MB-231, breast; HCT-116, colorectal; PC-3, prostate cancer), as well as one healthy human bronchial epithelial cell

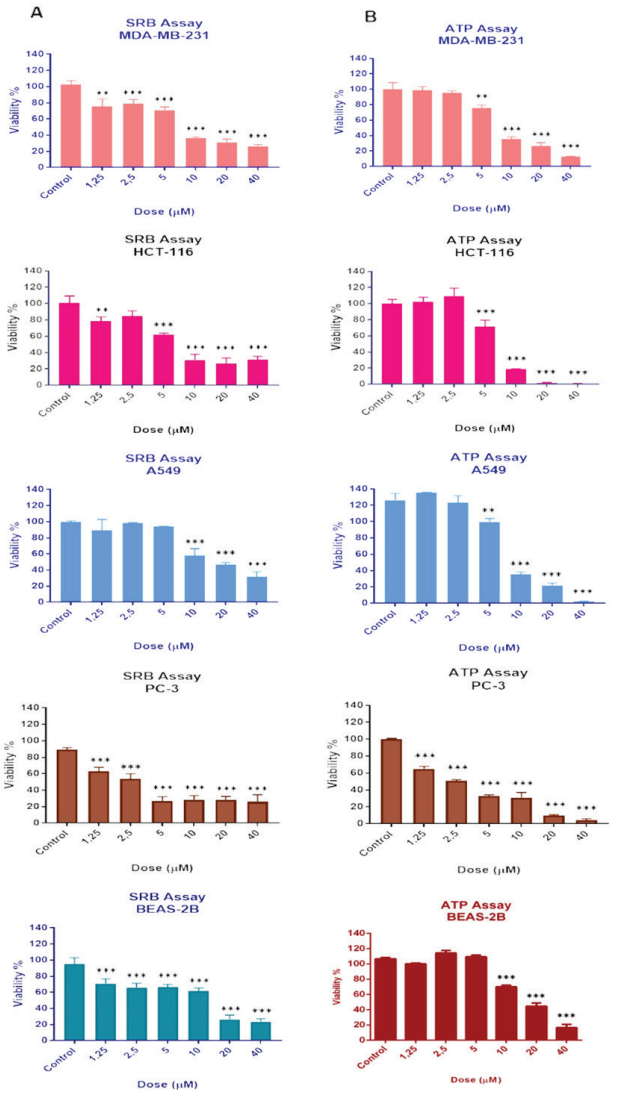


Figure 4. Measuring the effect of Complex 1 using the SRB (A) and ATP (B) assays. A549, PC-3, MDA-MB-231, HCT-116, and BEAS-2B cells were treated for 48 h at a concentration of 1.25-40 μM. *** $p < 0.001$. Data are presented as mean ± SD (n = 3).

line (BEAS-2B), for 48 h at various concentrations (1.25–40 µM; Figure 4). As a result of the SRB assays, Complex 1 significantly decreased the viability of all cell lines. Although Complex 1 showed a cytotoxic effect on all cell lines, it was effective at a much lower dose on the PC-3 cells. The IC_{50} (the concentration that kills 50% of cells) and IC_{90} (the concentration that kills 90% of cells) values were calculated with the results confirmed by the ATP assays (Table 1).

Table 1. IC_{50}, IC_{90} and, selectivity index values for Complex 1 calculated based on the results of the ATP assay with cells treated for 48 h. The SI was calculated for Complex 1 using the formula SI = (IC_{50} for normal cell line BEAS-2B) / (IC_{50} for the respective cancer cell line).

Complex 1	IC_{50} Dose (µM) ±	IC_{90} Dose (µM) ±	Selectivity Index (SI)
PC-3	2.6 ± 1.3	19.8 ± 0.4	1.15
MDA-MB-231	8.2 ± 0.6	> 40	0.37
A549	8.8 ± 1.2	32.2 ± 0.8	0.34
HCT-116	7.02 ± 0.9	15.1 ± 1.4	0.42
BEAS-2B	3.0 ± 1.6	> 40	-

The comparison of the IC_{50} results obtained from the different cancer cell lines with those of the cationic complexes has revealed the IC_{50} values presented here to be effective at much lower doses (28). That the dose that kills 90 % the cells is especially high in the healthy human bronchial epithelial cell line is noteworthy. While it is effective on cancer cells at lower doses, this low dose range is seen to be ineffective on healthy cells. These *in vitro* studies also need to be validated *in vivo*. Therefore, Complex 1 deserves further attention for its proof of concept in animal models. At the same time, the study compared the selectivity index (SI) values of Complex 1 tested on these cells. A favorable SI > 1.0 indicates a drug with efficacy against tumor cells greater than the toxicity against normal cells. Accordingly, the SI was observed to be particularly high in prostate cancer cells.

To investigate whether the cytotoxicity was caused by the complex or the ligand, the SRB assay was performed on the ligand only-treated cells. No cytotoxic effect of the ligand was observed in the SRB assay, as shown in another study (24). In order to certify the occurrence of cell death, a dose usage equivalent to IC_{90} is inevitable. Therefore, the IC_{90} dose was used for flow cytometry analysis to determine cell death and related parameters.

Apoptosis-inducing Effect of the Complex

The annexin V-FITC staining assay was carried out using the flow cytometer to further analyze whether or not the cell death mode was apoptosis. At 24h and 48h respectively, 14.65% and 14.95% of cells for A549, 35.45% and 46.58% of cells for MDA-MB-231, 11.35% and 18.50% of cells for PC-3, 35.7% and 50.55% of cells for HCT-116, and 15.45 % and 12.22% of cells for BEAS-2B underwent apoptosis (the total amount of both early and late-stage apoptosis; Figure 5). The complex has been shown to significantly induce apoptosis of the MDA-MB-231 and HCT-116 cell lines. However, the complex was found to induce cell death through primary necrosis for the A549, PC-3, and BEAS-2B cells. These findings clearly show Complex 1's ability to induce cell death through different pathways based on the cell line type.

Mitochondria are one of the regulators that have an important role in apoptosis. Membrane depolarization of mitochondria is an important marker for intrinsic apoptosis. After 24 h and 48 h of treatment with Complex 1 in all cell lines, a respective 41.3% and 97.15% of cells for A549, 41.35% and 95% for MDA-MB-231, 37.5% and 94.85% for PC-3, 34.85% and 95.95% for HCT-116, and 38.37% and 88.16% for BEAS-2B were found to be in state of mitochondria membrane-depolarization (Figure 6). Studies have reported mitochondrial membrane depolarization to increase in all cell lines based on time regardless of apoptosis or necrosis (29).

The decrease in Bcl-2 activity is related to the regulation of mitochondrial-mediated apoptosis and as a result, the change in activation of Bcl-2 was investigated regarding flow cytometry. To detect Bcl-2 inactivation after 24 h and 48 h of treatment with Complex 1 in all cell lines, the Bcl-2 inactivation assay was performed using the flow cytometer. Bcl-2 inactivation was found to be respectively 3.10% and 2.10% for A549, 40.6% and 54.70% for MDA-MB-231, 1.30% and 0.70% for PC-3, 8% and 72.80% for HCT-116, and 0.2% and 0% for BEAS-2B at the 24 h and 48 h marks (Figure S7). Since necrotic cell death occurred in the A549, PC-3, and BEAS-2B cells, no inactivation of Bcl-2 happened despite the mitochondrial membrane depolarization. In the MDA-MB-231 cell line, Bcl-2 inactivation further enhanced apoptosis in a time-dependent manner in addition to the mitochondrial membrane depolarization. Also, all these findings indicate that Complex 1 might have caused intrinsic apoptosis in MDA-MB-231. Similar to this, an increase in Bcl-2 inactivation occurred in the HCT-116 cell line as well, especially in the 48 hour application. This implies that Complex 1 may have a distinct killing effect that is based on cancer type.

γ.H2A.X activation is one of the significant markers that contribute to DNA damage. After double-strand breaks form in DNA, H2A.X is phosphorylated through the ATM and ATR pathways. The palladium-based complexes are well known for covalently bonding to DNA strands and causing DNA damage (30). To detect DNA damage after 24 h and 48 h of treatment with Complex 1 in all cell lines, the H2A.X activation assay was performed using the flow cytometer. H2A.X activation was found to respectively be 3.1% and 3.3% for A549, 19.7% and 34.5% for MDA-MB-231, 2.76% and 1.34% for PC-3, 44.8% and 39.7% for HCT-116, and 4% and 6.6% for BEAS-2B for the 24 h and 48 h cycles (Figure S8). While Complex 1-induced DNA damage was not detected in the A549, PC-3, or BEAS-2B cell

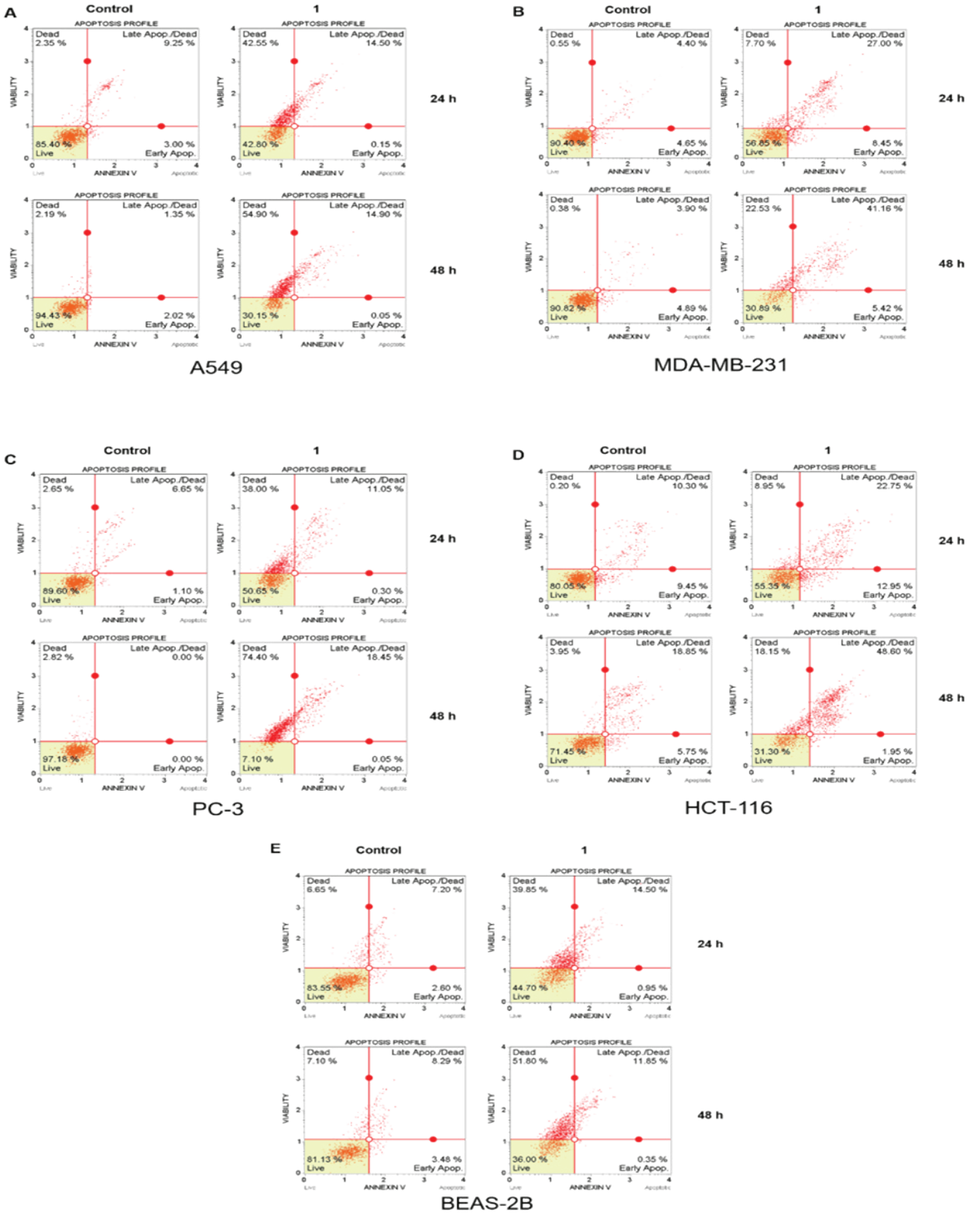


Figure 5. Assessment of phosphatidylserine translocation using flow cytometry. A549 (A), MDA-MB-231 (B), PC-3 (C), HCT-116 (D), and BEAS-2B (E) cells were treated with doses of Complex 1 at a concentration of IC_{90} for 24 h and 48 h.

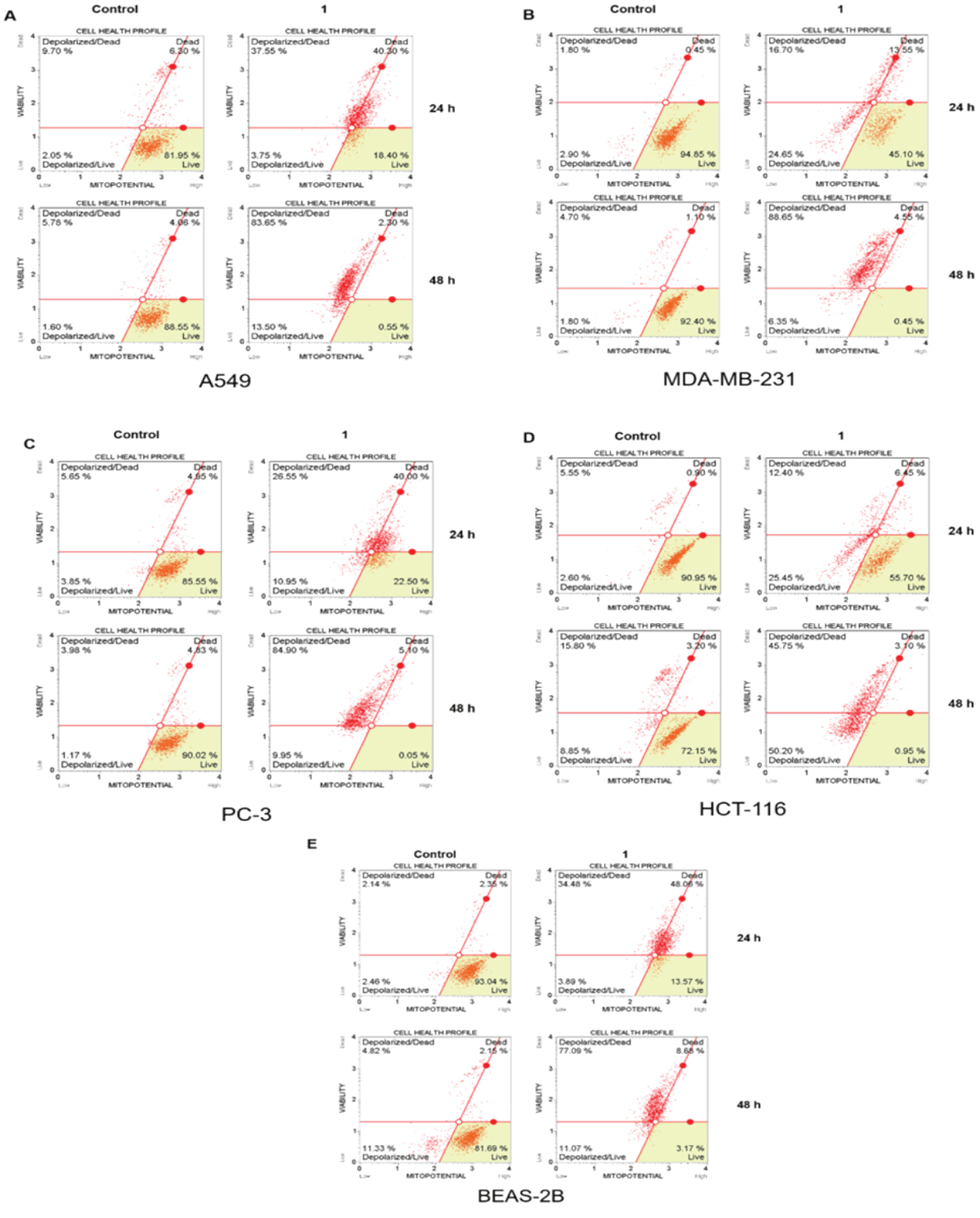


Figure 6. Mitochondria-dependent apoptosis in A549 (A), MDA-MB-231 (B), PC-3 (C), HCT-116 (D), and BEAS-2B (E) cells treated Complex 1 doses at a concentration of IC_{90} for 24 and 48 h.

lines, MDA-MB-231 and HCT-116 cell lines did show a time-dependent increase in DNA damage. This finding is particularly important, as these assays seem to confirm each other in terms of their role in the apoptotic process.

CONCLUSION

This study has synthesized and thoroughly characterized the cationic palladium(II) complex with N_4-donor tetradentate ligand using spectroscopic methods. The study also performed DFT calculations to obtain the optimized geometry. The palladium(II) adopted a significantly distorted square planar geometry with regard to Complex 1 due to the steric repulsion of the bulky benzimidazole chromophores in the 6,6'-positions of the 2,2'-bipyridine. Both the ligand and the palladium(II) complex are hydrated in a crystal form. The NMR and the FT-IR spectra of the complex show the ligand coordinates to the Pd center via imine N atoms to afford a doubly charged cationic complex.

When considering all these findings, Complex 1 seems to induce cell death by apoptosis through DNA damage and involvement of mitochondria in the HCT-116 and MDA-MB-231 cells while not having much of an effect in the other cell lines that were used. As such, Complex 1 may be considereds particularly effective against colon and triple-negative breast cancers. Therefore, Complex 1 as a novel palladium-based complex deserves to be studied further with regard to proof-of-concept studies on animal models.

Ethics Committee Approval: Ethics committee approval was not obtained because there was no use of human and animal data in this study.

Peer-review: Externally peer-reviewed.

Author Contributions: Conception/Design of Study - E.U., A.S., M.E.G., S.S.; Data Acquisition - E.U., A.S., M.E.G., S.S.; Data Analysis/Interpretation - E.U., A.S., M.E.G., S.S., I.Y.; Drafting Manuscript - M.E.G., R.O.A., E.U., A.S.; Critical Revision of Manuscript - I.Y., M.E.G., R.O.A., E.U., A.S.; Final Approval and Accountability - E.U., A.S., I.Y.

Conflicts of Interest: The authors declare no conflict of interest.

Financial Disclosure: This work was partly supported by the Turkish Scientific and Technical Research Council (TÜBİTAK) (grant number TBAG-2450(104T060)).

Acknowledgments: We gratefully acknowledge Nursel Açar Selçuki for carrying out computational DFT studies and we thank for the computer time on FenCluster (Ege University Faculty of Science).

REFERENCES

1. Phillips MC, Mousa SA. Clinical application of nano-targeting for enhancing chemotherapeutic efficacy and safety in cancer management. Nanomedicine 2022; 17(6): 405-21. [CrossRef]
2. Racané L, Zlatar I, Perin N, Cindrić M, Radovanović V, Banjanac M, et al. Biological Activity of Newly Synthesized Benzimidazole and Benzothizole 2, 5-Disubstituted Furane Derivatives. Molecules 2021; 26(16): 4935. [CrossRef]
3. Roopashree B, Gayathri V, Gopi A, Devaraju KS. Syntheses, characterizations, and antimicrobial activities of binuclear ruthenium (III) complexes containing 2-substituted benzimidazole derivatives. J Coord Chem 2012; 65(22): 4023-40. [CrossRef]
4. Renouard T, Fallahpour RA, Nazeeruddin MK, Humphry-Baker R, Gorelsky SI, Lever ABP, et al. Novel ruthenium sensitizers containing functionalized hybrid tetradentate ligands: synthesis, characterization, and INDO/S analysis. Inorg Chem 2002; 41(2): 367-78. [CrossRef]
5. Yau HC, Chan HL, Yang M. Determination of mode of interactions between novel drugs and calf thymus DNA by using quartz crystal resonator. Sens Actuators B Chem 2002; 81(2-3): 283-88. [CrossRef]
6. Heringova P, Kasparkova J, Brabec V. DNA adducts of antitumor cisplatin preclude telomeric sequences from forming G quadruplexes. J Biol Inorg Chem 2009; 14(6): 959-68. [CrossRef]
7. Büyükekşi SI, Orman EB, Şengül A, Altındal A, Özkaya AR. Electrochemical and photovoltaic studies on water soluble triads: Metallosupramolecular self-assembly of ditopic bis (imidazole) perylene diimide with platinum (II)-, and palladium (II)-2, 2': 6', 2 "-terpyridyl complex ions. Dyes Pig 2017; 144: 190-202. [CrossRef]
8. Largy E, Hamon F, Rosu F, Gabelica V, De PE, Guédin A, et al. Tridentate N-Donor Palladium (II) Complexes as Efficient Coordinating Quadruplex DNA Binders. Chemistry 2011; 17(47): 13274-283. [CrossRef]
9. Burda JV, Zeizinger M, Leszczynski J. Activation barriers and rate constants for hydration of platinum and palladium square-planar complexes: An ab initio study. J Chem Phys 2004; 120(3): 1253-62. [CrossRef]
10. Muller G, Bunzli, JCG, Schenk KJ, Piguet C, Hopfgartner G. Influence of bulky N-substituents on the formation of lanthanide triple helical complexes with a ligand derived from bis (benzimidazole) pyridine: structural and thermodynamic evidence. Inorg Chem 2001; 40(12): 2642-51. [CrossRef]
11. Cusumano M, Di Pietro ML, Giannetto A. Stacking surface effect in the DNA intercalation of some polypyridine platinum (II) complexes. Inorg Chem 1999; 38(8): 1754-58. [CrossRef]
12. Wong, ELM, Fang GS, Che CM, Zhu N. Highly cytotoxic iron (II) complexes with pentadentate pyridyl ligands as a new class of anti-tumor agents. Chem Commun 2005; (36): 4578-80. [CrossRef]
13. Davidson JP, Faber PJ, Fischer JrRG, Mansy S, Peresie HJ, Rosenberg B, et al. " Platinum-pyrimidine blues" and related complexes: a new class of potent antitumor agents. Cancer Chemother Rep 1975; 59(2 Pt 1): 287-300.
14. Yılmaz I, Akar OR, Erkisa M, Selvi S, Şengül A, Ulukaya E. Highly promising antitumor agent of a novel Platinum (II) complex bearing a tetradentate chelating ligand. ACS Med Chem Lett 2020; 11(5): 940-8. [CrossRef]
15. Drew D, Doyle JR, Shaver AG. Cyclic diolefin complexes of platinum and palladium. Inorg Syn 1972; 13: 47-55. [CrossRef]
16. Russo TV, Martin RL, Hay PJ. Density functional calculations on first-row transition metals. J Chem Phys 1994; 101(9): 7729-37. [CrossRef]
17. Hay PJ. Methods of Electronic Structure Theory: Plenum Press, 1977.
18. Dennington RD, Keith TA, Millam JM. GaussView 5.0, Gaussian. Inc., Wallingford, 20, 2008.
19. Zhang IY, Wu J, Xu X. Extending the reliability and applicability of B3LYP. Chem Commun 2010; 46(18): 3057-70. [CrossRef]
20. Czarnecki MA, Wojtków D. Effect of varying water content on the structure of butyl alcohol/water mixtures: FT-NIR two-dimensional correlation and chemometric studies. J Mol Struct 2008; 883: 203-8. [CrossRef]

21. Yılmaz I, Acar NS, Coles SJ, Şengül A. Spectroscopic, EPR, X-ray structural, and DFT studies of the complex compound of N4-donor ligand with copper (II). J Mol Struct 2020; 1214: 128204. [CrossRef]
22. Buyukeksi SI, Erkisa Genel M, Şengül A, Ulukaya E. Oral AY. Structural studies and cytotoxic activity of a new dinuclear coordination compound of palladium (II)-2, 2: 6, 2-terpyridine with rigid dianionic 1, 2, 4-triazole-3-sulfonate linker. Appl Organomet Chem 2018; 32(8): e4406. [CrossRef]
23. Lee C, Yang W, Parr RG. Development of the Colle-Salvetti correlation-energy formula into a functional of the electron density. Phys Rev B 1988; 37: 785-9. [CrossRef]
24. Kohn W, Sham LJ. Self-consistent equations including exchange and correlation effects. Phys Rev 1965; 140: A1133-8. [CrossRef]
25. Yurdakul Ş. Kurt M. Vibrational spectroscopic studies of metal (II) halide benzimidazole. J Mol Struct 2003; 650(1-3): 181-190. [CrossRef]
26. Bhattacherjee A, Wategaonkar S. Water bridges anchored by a C-H… O hydrogen bond: the role of weak interactions in molecular solvation. Phys Chem Chem Phys 2016; 18(40): 27745-49. [CrossRef]
27. Miao SB, Ji BM, Deng DS, Xu C, Ma N. Crystal structures and luminescence of two zinc (II) complexes with benzimidazole ligands. J Struct Chem 2010; 51(2): 386-91. [CrossRef]
28. Yıldız U, Şengül A, Kandemir I, Cömert F, Akkoç S, Coban B. The comparative study of the DNA binding and biological activities of the quaternized dicnq as a dicationic form and its platinum (II) heteroleptic cationic complex. Bioorg Chem 2019; 87: 70-7. [CrossRef]
29. Kim JS, He L, Lemasters JJ. Mitochondrial permeability transition: a common pathway to necrosis and apoptosis. Biochem Biophys Res Commun 2003; 304(3): 463-70. [CrossRef]
30. Kumar A, Naaz A, Prakasham AP, Gangwar MK, Butcher RJ, Panda D, Ghosh P. Potent anticancer activity with high selectivity of a chiral palladium N-Heterocyclic Carbene Complex. ACS omega 2017; 2(8): 4632-46. [CrossRef]

SUPPORTING INFORMATION

Differential Cytotoxic Activity of A New Cationic Pd(II) Coordination Compound with N_4-Tetradentate Hybrid Ligand in Cancer Cell Lines

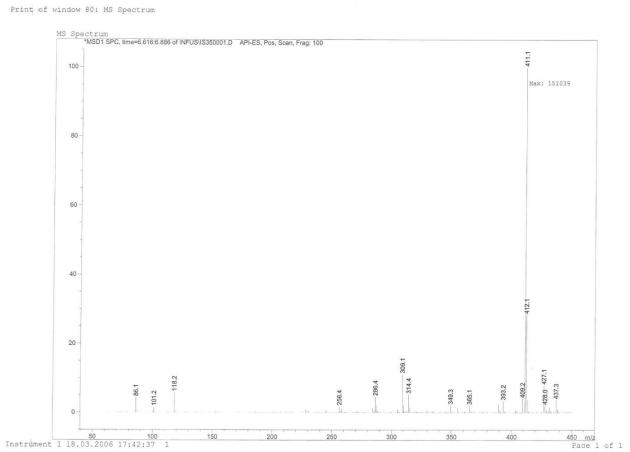


Figure S1. ESI-MS spectrum of **L**

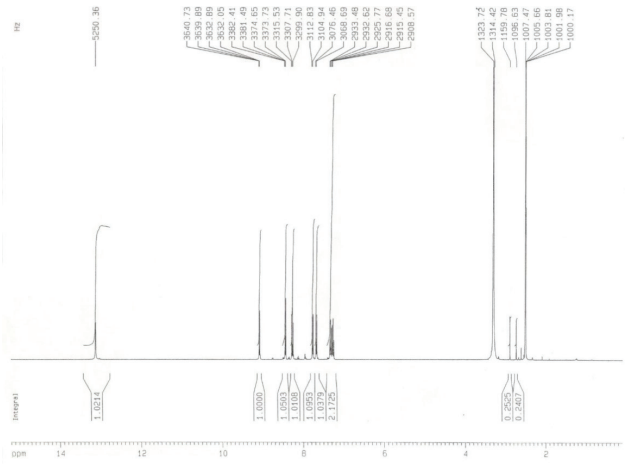


Figure S2. ^{1}H NMR spectrum of **L**

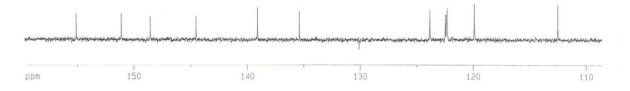


Figure S3. ^{13}C NMR spectrum of **L**

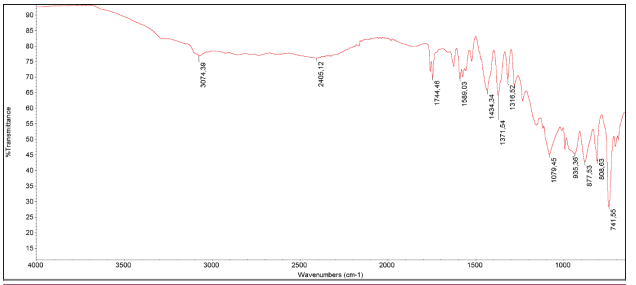


Figure S4. FT-IR (ATR) spectrum of **L**

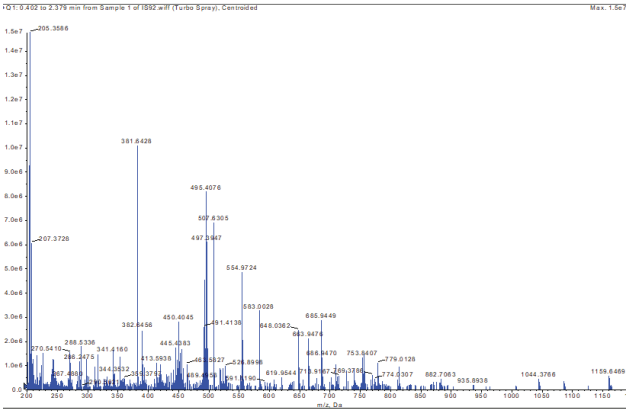


Figure S5. LC-ESI-MS spectrum of **1**

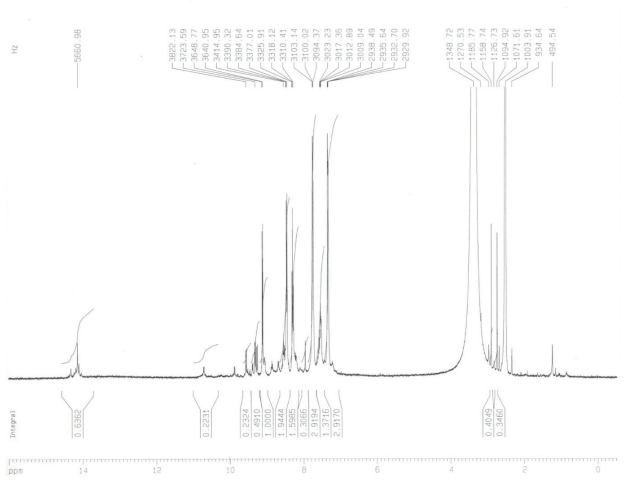


Figure S6. ^{1}H NMR spectrum of **1**

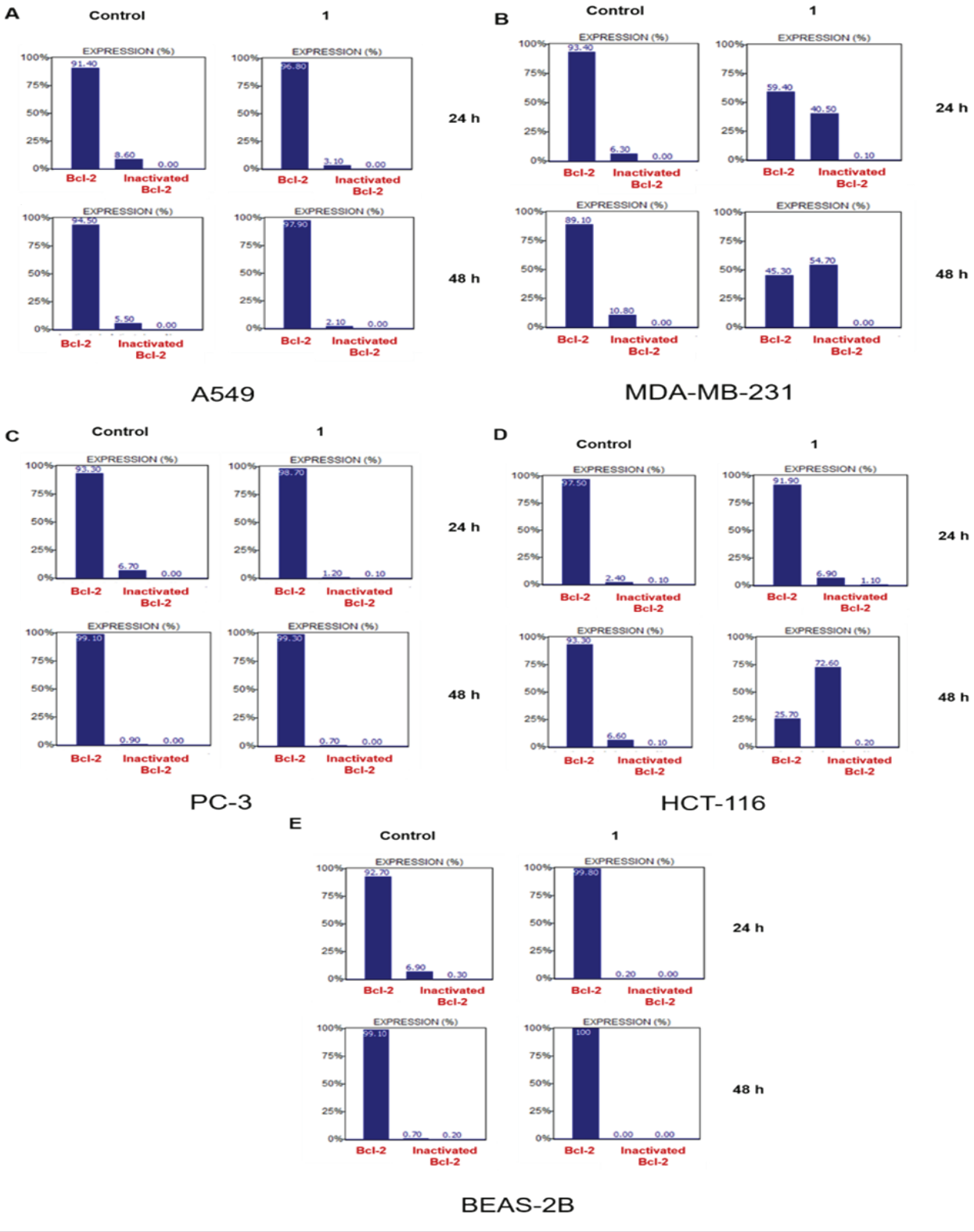


Figure S7. Bcl-2 phosphorylation (Ser70) in (A) A549, (B) MDA-MB-231, (C) PC-3, (D) HCT-116 and (E) BEAS-2B cell lines after treatment with complex 1 (IC_{90} doses) for 24 and 48 h.

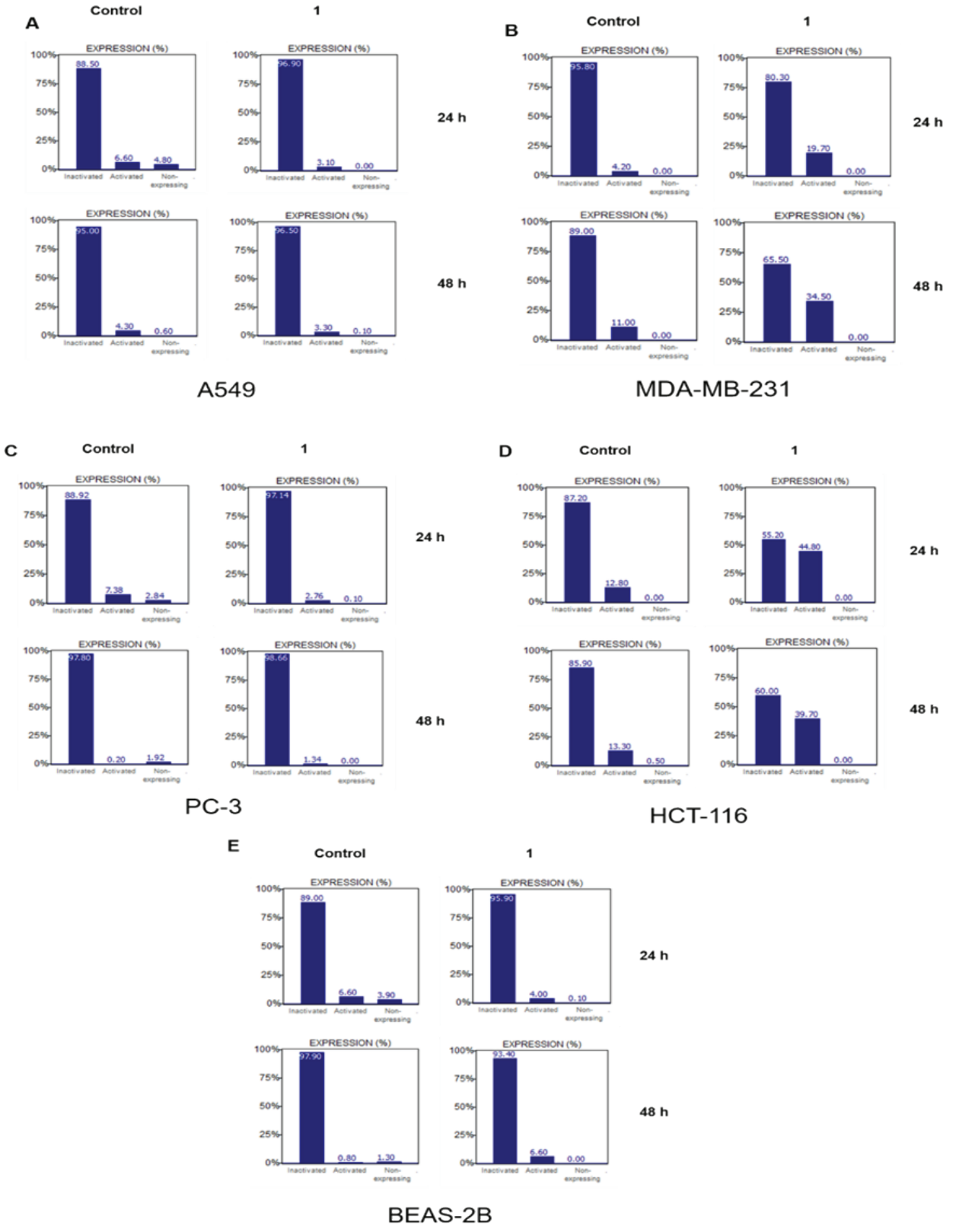


Figure S8. DNA damage in (A) A549, (B) MDA-MB-231, (C) PC-3, (D) HCT-116, and (E) BEAS-2B cell lines after treatment with complex 1 (IC_{90} doses) for 24 and 48 h.

Table S1. Calculated (in the gas phase) selected bond lengths (Å), angles (°), and dihedral angles for compound 1.

	Bond lengths (Å)		Angles(°)		Dihedral Angles(°)
Pd-N2	2.130	N2-Pd-N4	159.12	N2-Pd-N4-C1	168.25
Pd-N3	1.985	N3-Pd-N5	159.12	C17-N2-Pd-N5	7.99
Pd-N4	1.985	N2-Pd-N3	79.36	C16-C17-N2-Pd	4.00
Pd-N5	2.130	N3-Pd-N4	80.05	N2-C11-C10-N3	0.60
N2-C11	1.347	N4-Pd-N5	79.36	Pd-N2-C11-C10	-4.72
N2-C17	1.385	N2-Pd-N5	121.38	C17-N2-Pd-N4	-164.86
C17-C12	1.419	C11-N2-C17	106.68	C18-N5-Pd-N4	-174.59
C12-N1	1.384	C11-C10-N3	111.25	N4-C1-C24-N6	176.80
C12-C13	1.398	N3-C9-C10	119.14	N3-C10-C11-N1	176.80
C17-C16	1.403	C10-N3-C6	123.98		
C11-C10	1.458	N3-C6-C5	113.22		
C10-N3	1.347	C6-C5-N4	113.22		
N3-C6	1.356	C5-N4-C1	123.98		
C6-C5	1.484	N4-C1-C24	111.25		
C5-N4	1.356	C1-C24-N5	120.44		
N4-C1	1.347	N5-C24-N6	111.14		
C1-C24	1.458	C24-N5-C18	106.68		
C1-N5	1.347				
N5-C18	1.385				
C18-C23	1.419				
C23-N6	1.384				
C23-C22	1.398				
C18-C19	1.403				